

## The Ti-saturation surface for low-to-medium pressure metapelitic biotites: Implications for geothermometry and Ti-substitution mechanisms

DARRELL J. HENRY,<sup>1,\*</sup> CHARLES V. GUIDOTTI,<sup>2</sup> AND JENNIFER A. THOMSON<sup>3</sup>

<sup>1</sup>Department of Geology and Geophysics, Louisiana State University, Baton Rouge, Louisiana 70803, U.S.A.

<sup>2</sup>Department of Geological Sciences, University Of Maine, Orono, Maine 04469, U.S.A.

<sup>3</sup>Department of Geology, Sci 130, Eastern Washington University, Cheney, Washington 99004, U.S.A.

### ABSTRACT

The Ti content of biotite can serve as a geothermometer for graphitic, peraluminous metapelites that contain ilmenite or rutile and have equilibrated at roughly 4–6 kbar. The relationship between Ti-content, temperature, and Mg/(Mg + Fe) value was calibrated empirically using an extensive natural biotite data set (529 samples) from western Maine and south-central Massachusetts in combination with the petrogenetic grid of Spear et al. (1999). The calculated Ti-saturation surface is curved such that for a given Mg/(Mg + Fe) value, Ti concentration increases as a function of temperature in a nonlinear fashion, and for a given temperature Ti concentrations decrease with an increase in Mg/(Mg + Fe). The fit to the Ti-saturation surface can be reformulated as the geothermometric expression:  $T = \{[\ln(\text{Ti}) - a - c(X_{\text{Mg}})^3]/b\}^{0.333}$ , in which  $T$  is temperature in degrees Celsius, Ti is the number of atoms per formula unit (apfu) normalized on the basis of 22 O atoms,  $X_{\text{Mg}}$  is Mg/(Mg + Fe),  $a = -2.3594$ ,  $b = 4.6482 \times 10^{-9}$  and  $c = -1.7283$ . The calibration range for this expression is  $X_{\text{Mg}} = 0.275\text{--}1.000$ ,  $\text{Ti} = 0.04\text{--}0.60$  apfu, and  $T = 480\text{--}800$  °C. Precision of the Ti-in-biotite geothermometer is estimated to be  $\pm 24$  °C at the lower temperature range and improves to  $\pm 12$  °C at higher temperatures. Application of the Ti-in-biotite geothermometer to ilmenite- or rutile-bearing, graphitic, peraluminous metapelites equilibrated at 3–6 kbar is generally consistent with independent temperature determinations, but with some deviations that represent local reequilibration. Consequently, the Ti systematics in biotite can also serve as the basis of a very sensitive indicator of chemical equilibrium, or lack thereof. Application of the geothermometer to metapelites not containing the requisite mineral assemblages can lead to minor-to-significant errors in estimated temperatures.

Biotite Ti-substitution mechanisms are controlled by several factors. Based on the biotite calibration data set, magnesian biotites ( $X_{\text{Mg}} > 0.65$ ) incorporate Ti in accordance with the exchange vector  $\text{TiAl}_2\text{R}_{-1}\text{Si}_{-2}$ , where R is the sum of the divalent cations Mg + Fe + Mn. This substitution mechanism is primarily a response to misfit of the octahedral and tetrahedral layers in magnesian biotites. Intermediate biotites ( $X_{\text{Mg}} < 0.65$ ), particularly at higher temperatures, exhibit enhanced Ti concentrations, most consistent with the Ti-deprotonation  $\text{TiO}_2\text{R}_{-1}(\text{OH})_{-2}$  exchange vector. Dominance of Ti-deprotonation substitution is largely a function of reduction of  $\text{H}_2\text{O}$  activity at higher metamorphic grades. Supplementary biotite data from metaluminous amphibolites and mafic granulites, metamorphosed isothermally with variable  $\text{H}_2\text{O}$  activities, reveal that low-Al biotite incorporates significantly higher concentrations of Ti relative to peraluminous biotite as a result of a combination of the exchange vectors  $\text{TiO}_2\text{R}_{-1}(\text{OH})_{-2}$  and  $\text{RSiAl}_2$  substituting in roughly an 8:1 ratio.

### INTRODUCTION

The concentration of Ti in biotite has long been considered to be a function primarily of changing temperature conditions in metamorphic rocks and has been suggested as a potential geothermometer (Engel and Engel 1960; Kwak 1968; Robert 1976; Dymek 1983; Patiño Douce 1993). However, the factors that influence the incorporation of Ti in biotite are more multifaceted than simple temperature change, and involve a relatively complex interplay among temperature, pressure, biotite crystal chemistry, and coexisting mineral assemblages (Guidotti et al. 1977, 1988;

Dymek 1983; Labotka 1983; Guidotti 1984; Tracy and Robinson 1988; Guidotti and Sassi 2002; Henry and Guidotti 2002).

Experimental investigators have examined how temperature, pressure, and composition control the amount of Ti in biotite. The temperature effect appears to be the most influential. In phlogopite, the incorporation of Ti is relatively dramatic at high temperatures, particularly higher than 800 °C. For instance, Robert (1976) found that Ti solubility is relatively low, 0.07 Ti atoms per formula unit (apfu), at 600 °C and 1 kbar, but increases significantly to 0.2 Ti apfu at 800 °C and 1 kbar, and to 0.7 Ti apfu at 1000 °C and 1 kbar. Increasing pressure has the opposite effect, with Ti concentrations decreasing substantially with increasing pressure (Forbes and Flower 1974; Robert 1976;

\* E-mail: dhenry@geol.lsu.edu

Arima and Edgar 1981; Tronnes et al. 1985). Robert (1976) noted that at 1000 °C, a pressure increase from 1 to 7 kbar results in a decrease in Ti concentration in phlogopite from 0.7 Ti apfu to 0.2 Ti apfu. Early experiments also demonstrated a compositional influence such that Ti content in biotite generally increases with an increase in Fe content (Arima and Edgar 1981; Abrecht and Hewitt 1988). Combinations of these parameters can have a profound effect on Ti content in biotite. For instance, Patiño Douce and Johnston (1991), examining Ti concentrations in intermediate Fe-Mg biotite from a series of partial-melting experiments of natural peraluminous metapelites, found that at 825–975 °C and 7–13 kbar, Ti increases with temperature in a non-linear fashion. Based on these experiments, Patiño Douce (1993) calculated the pressure effect on Ti concentrations in intermediate Fe-Mg ( $X_{Mg} = 0.5$ ) biotite coexisting with orthopyroxene, K-feldspar, and quartz. He estimated that a pressure increase from 5 to 15 kbar causes a decrease of Ti by 0.24 apfu at 900 °C, by 0.10 apfu at 800 °C, and by 0.02 apfu at 700 °C.

Despite these previous studies, it is difficult to apply experimental findings to the spectrum of *P-T* conditions, bulk compositions, and mineral assemblages found in metamorphic and igneous rocks. A better understanding of this complex relationship is needed. An important result of the present study is the illustration of how careful investigations of biotite in well-constrained natural systems can further elucidate aspects of the experimental studies and provide an independent means to investigate additional factors that influence Ti concentrations in biotite.

Henry and Guidotti (2002) studied Ti concentrations in biotite from metapelitic rocks in a geologically and petrologically well-characterized terrane associated with the Acadian Orogeny of western Maine. They investigated biotite in metapelitic rocks in the garnet through sillimanite-K-feldspar zones at roughly isobaric conditions of about 3.3 kbar, based on the petrogenetic grid of Spear and Cheney (1989). Their extensive natural biotite data set (>450 analyses) from thoroughly equilibrated metapelitic schists of western Maine exhibits systematic variations in Ti contents over a continuum of metamorphic grade and biotite mineral chemistry. To limit the number of competing substitutions in biotite, Henry and Guidotti (2002) focused on samples with selected mineral assemblages. They studied pelitic schists that contained quartz, aluminous minerals (chlorite, staurolite or sillimanite), Ti minerals (ilmenite or rutile), and graphite. In such schists, Si, Al, and Ti in biotite are near or at saturation levels for a given temperature, and the effect of variable bulk composition is limited. The occurrence of graphite in the metapelitic schists restricts the metapelites to low and fairly constant  $f_{O_2}$ . Consequently, biotites contain low and roughly constant amounts of Fe<sup>3+</sup> (~12% of Fe<sub>total</sub>) (Guidotti and Dyar 1991). At the same time, the biotites studied by Henry and Guidotti (2002) have a relatively wide range of Mg/(Mg + Fe) ratios controlled by sulfide-silicate interactions (Henry 1981; Guidotti et al. 1988). Henry and Guidotti (2002) estimated the equilibration temperature for each sample by noting its position relative to mapped isograds. Isograd temperatures themselves were derived from the Spear and Cheney (1989) petrogenetic grid for metapelites assuming 3.3 kbar. Based on the inferred temperature and biotite chemistry, they were able to calculate a

3.3 kbar Ti-saturation surface for natural biotite as a function of temperature and Mg/(Mg + Fe) values.

One implication of the Henry and Guidotti (2002) investigation is that a Ti-in-biotite geothermometer can be formulated from the surface-fit expression of the Ti-saturation surface. However, this geothermometer is strictly valid only for biotite from metapelites that: (1) have mineral assemblages similar to those of the calibration samples; (2) equilibrated at roughly 3.3 kbar; and (3) fall within the range of biotite compositions and temperatures of the calibration samples. Because of the ubiquitous nature of biotite in many rock types, further development of this potential single-mineral thermometer is warranted. So, this paper considers geothermometric aspects of the biotite Ti-saturation surface in a more general sense, defines compositional and textural manifestations of biotite disequilibrium or local equilibrium, and examines likely Ti-substitution mechanisms in biotite in a crystallochemical and petrologic context.

### BIOTITE DATA SETS

The biotite data considered in this study include the original Henry and Guidotti (2002) data set as well as supplementary data from Maine and south-central Massachusetts. Biotite data from Massachusetts are especially useful because they developed at higher temperature and slightly higher pressure conditions. For all biotites, we redetermined metamorphic pressures and temperatures using the updated petrogenetic grid of Spear et al. (1999). The updated petrogenetic grid was used because it provides improved consistency among a variety of natural metapelitic mineral assemblages (Pattison et al. 2002).

#### Maine data set

The biotite-bearing samples from western Maine are primarily from metamorphosed Ordovician-Devonian strata that were extensively metamorphosed in the Siluro-Devonian Acadian Orogeny (Osberg et al. 1985; Guidotti 1989). The Acadian metamorphism involves regionally developed recrystallization with grades ranging from subgreenschist-facies to upper amphibolite-facies (Guidotti 1989). The polymetamorphic history includes an initial greenschist-facies regional metamorphism (M1), and regional/contact metamorphic overprints (M2 and M3) that are largely postkinematic. Further details of the metamorphic history are presented in Guidotti (1970a, 1970b, 1974, 1985, 1989), Henry (1981), Holdaway et al. (1982, 1988), deYoreo et al. (1989), Pressley and Brown (1999); Henry and Guidotti (2002), and Johnson et al. (2003). Of special importance is the observation that in the specific area considered by Henry and Guidotti (2002) (see their Fig. 1), the M3 metamorphism is the dominant metamorphic overprint and that minerals in the metapelites across that region thoroughly equilibrated under nearly isobaric conditions (Guidotti 1989; Henry and Guidotti 2002).

These western Maine samples come primarily from the Rangeley, Oquossoc, Rumford, and Old Speck Mtn. 15' quadrangles. In this region, the isograd pattern in metapelitic schists roughly follow the outlines of the intruding pluton borders, and developed during the M3 metamorphic overprint. Based on the isograds, Guidotti et al. (1988) and Guidotti and Dyar (1991) defined 4 major zones (garnet, staurolite, sillimanite, and sillimanite-K-feldspar) (Table 1). They divided several of the zones

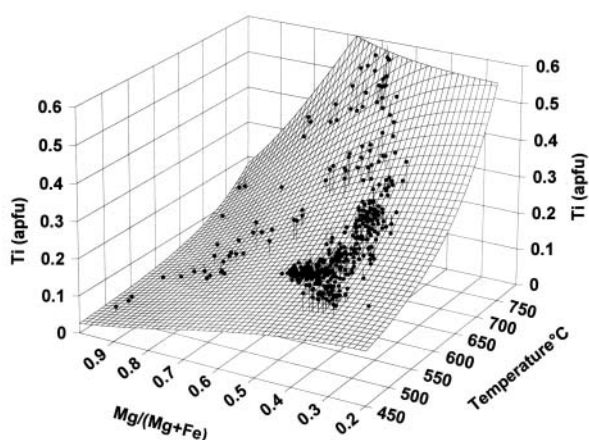


FIGURE 1. Titanium saturation surface for natural peraluminous biotites at 4–6 kbar. Perspective view of the surface highlights the influence of Mg content on Ti. Vertical lines connect individual data points above and below the fitted surface. This biotite data set does not include values of Ti > 0.6 apfu and Mg/(Mg + Fe) < 0.275.

TABLE 1. Temperature constraints for graphitic, aluminous, biotite-bearing metapelite samples from western Maine and south-central Massachusetts

Zone no.	Zone name	Isograd reaction	T °C (4 kbar)*	T °C (6 kbar)*
1	Lower Grt		(495)	
2	Middle Grt		(515)	
3	Upper Grt		(535)	
4	Lower St	Grt + Chl = St + Bt	545	
5	Upper St		(555)	
6	Transition	St + Chl = Bt + Sil	580	615
7	Lower Sil		(600)	
		St = Grt + Bt + Sil	620	655
8	Upper Sil		(640)	(665)
9	Lower Sil-Kfs	Ms = Kfs + Sil	660	680
10	Upper Sil-Kfs		(685)	(705)
DMZ† no.	Zone name	Dehydration melt reaction		
DM1	Ms melt	Ms + Ab = Sil + Kfs + melt	650	650
DM2	Bt-Grt-Crd melt	Bt + Sil = Grt + Crd + melt	715	775
DM3	Bt-Opx-Crd melt	Bt + Grt = Opx + Crd + melt	795	825

\* Temperatures are based on locations of isograd reactions and dehydration melting reactions at 4 and 6 kbar calibrated against the Spear et al. (1999) petrogenetic grid. The temperatures in parentheses represent the estimated temperature in the middle of each zone. Abbreviations: Ab = albite; Bt = biotite, Chl = chlorite, Crd = cordierite, Grt = garnet, Kfs = K-feldspar, Ms = muscovite, Sil = sillimanite and St = staurolite.

† Dehydration melting zone number. This represents the temperature of major discontinuous dehydration melt reactions in metapelitic rocks as defined by Spear et al. (1999).

into lower, middle, and upper portions based on progressive changes in textures and compositions of muscovite, biotite, and chlorite from specific limiting assemblages (Guidotti et al. 1988, 1991). This approach resulted in 10 mappable metamorphic zones that were used to assign temperatures to individual samples by calibrating the isograd reactions against the Spear et al. (1999) petrogenetic grid at 4 kbar and interpolating temperatures based on the relative position with metamorphic zones (Table 1).

Besides the Henry and Guidotti (2002) data, literature sources (see below) provided additional metapelitic biotite data (29 analyses) from south-central Maine so we could extend the temperature and compositional range of our study. A subset of biotite data came from Ferry (1981), who examined graphitic

sulfide-rich schists that equilibrated under similar pressure conditions to those of western Maine. The data of Ferry include several Mg-rich biotites from pelites similar to those of the western Maine samples, but for lower grade (biotite and garnet zone) conditions (480–520 °C). Additional data came from Dutrow (1985), who studied biotite to upper sillimanite zone metapelites that have appropriate mineral assemblages, and include some relatively Fe-rich biotites [Mg/(Mg + Fe) = 0.275].

### South-central Massachusetts data set

Biotite data (50 analyses) from south-central Massachusetts broaden our study to higher temperatures of 680–800 °C (Tracy 1978; Tracy and Robinson 1988; Peterson 1992; Thomson 1992, 2001). Several of the metapelite samples exhibit sulfide-silicate reactions, thereby extending the biotite range to more magnesian compositions [Mg/(Mg + Fe) = 0.43–1.00] (Tracy and Robinson 1988). The Massachusetts samples are from the Silurian and Devonian metasedimentary rocks of the Kearsarge-Central Maine Synclinorium of south-central Massachusetts that were intensely deformed and metamorphosed during the Acadian Orogeny. Pelitic gneisses, cordierite-garnet pegmatites, and leucocratic garnetiferous melt segregations are found in this upper amphibolite to granulite-facies terrane. The metamorphic zones include the upper sillimanite, lower sillimanite-K-feldspar, upper sillimanite-K-feldspar, muscovite melt, and biotite-garnet-cordierite melt zones (Table 1). The latter zone is a consequence of a discontinuous biotite dehydration melting reaction (DM2). The Massachusetts biotite data were used for calibration purposes only if the biotite data were derived from graphitic, peraluminous, and Ti-saturated metapelitic rocks similar to the western Maine metapelites. Additionally, because of the possibility of significant reequilibration associated with fluid released from local crystallization of melts, biotite data were restricted to samples that do not exhibit significant intergranular compositional heterogeneity among biotite grains in the same sample. The most recent pressure estimate for the peak metamorphism is 6–7 kbar following a counterclockwise *P-T* path (Thomson 2001). We estimated peak metamorphic temperatures using the petrogenetic grid of Spear et al. (1999) assuming a pressure of 6 kbar.

## RESULTS

### Ti-saturation surface

To obtain the optimal fit of the biotite data, we normalized the biotite formulae on a 22 O-atom basis assuming all Fe as Fe<sup>2+</sup> to calculate Ti atoms per formula unit (apfu). We then fit the entire data set, containing 529 biotite analyses, to equations that relate Ti in peraluminous biotites at 4–6 kbar to *T* °C and Mg/(Mg + Fe) values. More than 500 candidate surface-fit equations were tried using the TableCurve3D software. All data were given equal weighting. Candidate fit equations were sorted by the F-statistic criterion (ratio of the mean squared regression to the mean squared error) to optimize the surface fit while maintaining simplicity of form of the equation. Using this criterion, the optimal surface-fit equation is:

$$\ln z = a + bx^3 + cy^3 \quad (1)$$

where  $x = T$  °C,  $y = \text{Mg}/(\text{Mg} + \text{Fe})$ , and  $z = \text{Ti}$  (apfu).

Table 2 gives values for  $a$ ,  $b$ , and  $c$  and several statistical parameters for the fit. Figure 1 is a three-dimensional projection of the data and fitted surface. The fit to the data is excellent, having a correlation coefficient ( $r^2$ ) of 0.924. The additional data and updated temperature estimates used in this study resulted in a significantly improved fit relative to the previous results of Henry and Guidotti (2002) who obtained an  $r^2$  of 0.866 for the fit. An encouraging aspect of this fit is that the Ti-saturation surface, although being derived from natural data, is consistent with the general Ti trends observed in the biotite experiments discussed earlier.

Figure 2 shows isotherms projected on a Ti vs.  $Mg/(Mg + Fe)$  diagram for biotite. This projection provides an instructive way of viewing the influence of temperature on biotite chemistry in Ti-saturated metapelites. Isotherms are relatively closely spaced at temperatures below about 600 °C, and at more magnesian compositions. Because our data only covers Ti values ranging from 0.04 to 0.60 apfu,  $Mg/(Mg + Fe)$  values from 0.275 to 1.000, temperatures of 480 to 800 °C, and pressures of 4 to 6 kbar, extrapolation of isotherms beyond these ranges may introduce significant error. By calculating a temperature using Equation 2 (below) for each of the calibration data points and determining its deviation relative to the fitted saturation surface, we are able to estimate the accumulated uncertainties for different segments of the surface. The calculated temperatures are within  $\pm 24$  °C of the saturation surface in the range of 480–600 °C,  $\pm 23$  °C in the range 600–700 °C, and  $\pm 12$  °C in the range 700–800 °C. The standard deviations in the different ranges are considered measures of precision of the fit of the surface, being accumulated uncertainties associated with analytical precision and assignment of correct

temperature and pressure to individual samples. Although the accuracy of the Ti-saturation surface is related to the quality of the fitted surface, it is principally a function of the accuracy of the positions of the isogradic reactions in the Spear et al. (1999) petrogenetic grid. However, slight shifts in the locations of the isogradic reactions will not have significant effects on the general shape of the biotite Ti-saturation surface.

### Single mineral Ti-in-biotite geothermometer

Using Equation 1, we can derive a single-mineral Ti-in-biotite geothermometer for peraluminous biotites in metapelites equilibrated at 4–6 kbar. Temperatures can be determined either by plotting biotite Ti and  $Mg/(Mg + Fe)$  values on Figure 2 or by calculating temperatures directly from the expression:

$$T = \{[\ln(\text{Ti}) - a - c(X_{\text{Mg}})^3]/b\}^{0.333} \quad (2)$$

where  $T$  is temperature in °C, Ti is the apfu normalized to 22 O atoms,  $X_{\text{Mg}}$  is  $Mg/(Mg+Fe)$ , and the  $a$ ,  $b$ , and  $c$  parameters are given in Table 2. This expression is valid in the range  $X_{\text{Mg}} = 0.275$ –1.000,  $\text{Ti} = 0.04$ –0.60 apfu and  $T = 480$ –800 °C. Based on the accumulated uncertainties of the determination of the Ti-saturation surface, the precision of the Ti-in-biotite geothermometer is estimated to be  $\pm 24$  °C at lower temperatures (<600 °C), improving to  $\pm 12$  °C at high temperature (>700 °C). The accuracy of the Ti-in-biotite geothermometer, being primarily a function of the accuracy of the Spear et al. (1999) petrogenetic grid, is difficult to assess quantitatively, but Ti-in-biotite temperatures generally agree with independently determined temperature estimates to within 25 °C (see below).

## DISCUSSION

The systematics of Ti in peraluminous biotite not only permits calibration of a Ti-in-biotite geothermometer, but also gives us convenient criteria for detecting deviation from chemical equilibrium of individual biotite grains. Furthermore, the calibration biotite data set will give us insights into Ti-substitution mechanisms across the range of peraluminous biotites at different temperatures and will reveal the manner in which biotite chemistry is influenced by metamorphic conditions. Finally, we will use an additional biotite data set from metaluminous metamorphic rocks to examine the way that Ti substitution responds to different bulk compositions.

### Ti-in-biotite geothermometer: application to natural peraluminous metapelites

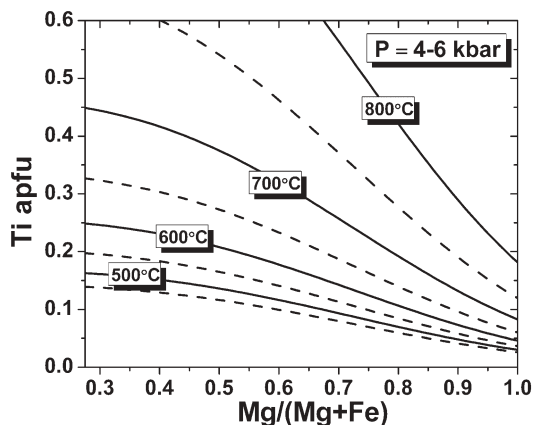
The accuracy of the Ti-in-biotite geothermometer can be assessed if well-constrained temperature estimates, obtained by independent geothermometers or petrogenetic grids, are available. Significant disagreements between the temperature estimates may reveal either: (1) inadequacy of the equation used to fit our calibration data; (2) a problem with the independent temperature estimate; (3) inappropriate extrapolation of the Ti-in-biotite geothermometer outside of its calibration range; or (4) alteration, disequilibrium, local equilibrium, or reequilibration of the biotite following the peak temperature conditions. The latter factor can be particularly subtle.

Figure 3 compares temperature estimates from the original lit-

**TABLE 2.** Summary of surface-fit equation coefficients and statistical parameters\* for the full biotite data set using the equation  $\ln z = a + bx^3 + cy^3$

Coefficient	Value	Standard error	95% confidence limits
a	-2.3594	0.0141	-2.3870 to -2.3317
b	4.6482e-9	5.1970e-11	4.5461e-9 to 4.7503e-9
c	-1.7283	0.0584	-1.8432 to -1.6134

\* This surface-fit equation has a coefficient of determination ( $r^2$ ) of 0.924 for these data, where  $r^2 = 1 - (\text{SSE}/\text{SSM})$ . SSE is the sum of the squares due to error and SSM is the sum of the squares about the mean.



**FIGURE 2.** Temperature isotherms (°C) calculated from the surface-fit equation on a Ti vs.  $Mg/(Mg + Fe)$  diagram. The dashed curves represent the intermediate 50 °C interval isotherms.

erature source with temperatures obtained using the Ti-in-biotite geothermometer. There is a favorable agreement between these independent temperature estimates, but there are some noteworthy deviations. For discussion purposes it is convenient to divide the data into 3 general groupings of metamorphic environments: low-pressure contact metamorphic aureoles, lower-to-middle amphibolite-facies regional metamorphic settings, and upper amphibolite- to granulite-facies regional metamorphic settings.

**Low-pressure contact metamorphic aureoles.** Several relatively low pressure terranes (3–3.5 kbar) contain graphitic, biotite-bearing peraluminous metapelites associated with contact metamorphic aureoles. Biotite from a series of 26 metapelites containing ilmenite or rutile is reported from the 3 kbar Ballachulish contact metamorphic aureole, Scotland (Pattison 1985, 1987, 1989, 1991, unpublished data; Pattison and Harte 1991; Pattison et al. 2002). Application of the Ti-in-biotite geothermometer gives temperatures that average  $16 \pm 23$  °C higher than the estimated temperatures of 550–630 °C. Symmes and Ferry (1995) characterized 4 representative biotites from the andalusite-cordierite to leucocratic-veining zones in the high-level Onawa Contact Aureole, Maine. Over the temperature range of 519–643 °C, the Ti-in-biotite temperatures are within  $\pm 24$  °C of their estimated temperatures. Porphyroblastic peraluminous schists in the thermal aureole of the Victor Harbor Granite, South Australia, preserve a record of mineral growth consistent with a counterclockwise *P-T* path. Maximum temperatures of 580 °C were reached at  $\sim 3$  kbar before pressure increased to  $\sim 4$  kbar with a concurrent decrease in temperature to  $\sim 560$  °C, as suggested by late mineral growth (Alias et al. 2002). The Ti-in-biotite geothermometer applied to 6 samples gives similar temperatures with an average value of  $570 \pm 16$  °C.

**Lower-to-middle amphibolite facies regional metamor-**

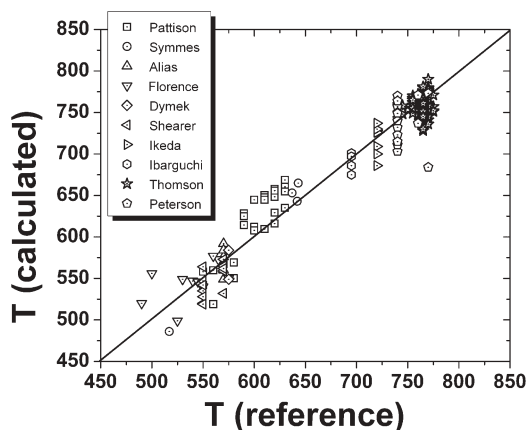


**FIGURE 3.** Calculation of Ti-in-biotite temperatures for graphitic, peraluminous metapelites with ilmenite and/or rutile for areas that are 3–6 kbar. *T* (reference) represents the temperature (°C) from the literature source. *T* (calculated) represents the calculated Ti-in-biotite temperature (°C). The solid line is reference line with a slope of 1. The literature sources include Ibarguchi and Martinez (1982), Dymek (1983), Pattison (1985, 1987, 1989, 1991, unpublished data), Shearer et al. (1986), Pattison and Harte (1991), Peterson (1992), Thomson (1992, 2001), Florence et al. (1993), Symmes and Ferry (1995), Ikeda (1998a), Alias et al. (2002), and Pattison et al. (2002).

**phic settings.** Peraluminous schists from the Bronson Hill anticlinorium of New Hampshire equilibrated at 3.8–6.6 kbar and 490–575 °C according to Florence et al. (1993). Ten biotite analyses give Ti-in-biotite temperatures slightly deviating ( $-8 \pm 25$  °C) from the Florence et al. values. Biotites from amphibolite-facies peraluminous schists from Itivdlinguaq, Greenland (Dymek 1983) give Ti-in-biotite temperatures of  $566 \pm 24$  °C consistent with original estimates of 575 °C. Peraluminous metapelites from the staurolite zone and transitional sillimanite zone of the contact aureole associated with the Harney Peak Granite of the Black Hills, South Dakota equilibrated at about 550–570 °C and 3.5–4.5 kbar (Shearer et al. 1986), and have biotites that yield Ti-in-biotite temperatures of  $536 \pm 16$  °C (staurolite zone) and  $553 \pm 16$  °C (transition zone). Eight samples from the garnet-cordierite zone ( $\sim 720$  °C, 4–5 kbar), the highest-grade zone in a regional-contact metamorphic aureole from the Ryoke metamorphic rocks in the Yanai district of SW Japan (Ikeda 1998a), have biotites with Ti-in-biotite temperatures of  $712 \pm 20$  °C. Biotite inclusions in K-feldspar in this high-grade zone are consistently Ti-richer than matrix biotites and give Ti-in-biotite temperatures 29–35 °C higher than matrix biotites, implying continued reequilibration of the matrix on cooling from higher temperature conditions.

**Upper amphibolite- to granulite-facies regional metamorphic settings.** Application of the Ti-in-biotite geothermometer to high-grade metapelites generally agrees with the independent temperature estimates, but there are some significant deviations reflecting retrogression of biotite or local departures from equilibrium. Garnet-cordierite-sillimanite gneisses from the El Tormes Thermal Dome, Spain are estimated to have equilibrated at 695 °C, 4.3 kbar (Ibarguchi and Martinez 1982) and have matrix biotites that have Ti-in-biotite temperatures of  $687 \pm 12$  °C. The high-grade metapelites from south-central Massachusetts not only contain samples that displayed significant intergranular homogeneity that were used as part of the calibration data set, but also have samples that exhibit significant intergranular heterogeneity and were excluded from the calibration (Thomson 1992, 2001; Peterson 1992). The results of their entire biotite data set, including matrix brown biotite and brown biotite proximal to other mafic phases, are plotted on Figure 3. Data from 112 individual analyses illustrate that deviations can be significant, signaling some compositional resetting. Similar deviations appear relatively common in many high-grade, melt-bearing metapelites (e.g., Graessner and Schenk 2001; Moraes et al. 2002). The wide range in biotite chemistry commonly found within individual high-grade metapelite samples will be discussed further when biotite re-equilibration is considered.

**Peraluminous metapelites without a Ti-saturating mineral and/or graphite.** As expected, application of the Ti-in-biotite geothermometry from peraluminous metapelites without Ti-saturating minerals (ilmenite or rutile) generally results in moderate to large temperature underestimates. For example, biotite data from 4 samples of magnetite-bearing, biotite-sillimanite schists and garnet-cordierite gneisses from South Africa yield Ti-in-biotite temperatures  $61 \pm 12$  °C below the 750 °C estimate of Waters and Whales (1984). Additionally, melting experiments (6 kbar, 750–900 °C) of Patiño Douce and Harris (1998), using natural peraluminous schists with no reported Ti-saturating min-

erals in the starting materials or experimental products, contain biotites that yield Ti-in-biotite temperatures that underestimate the experimental temperatures by  $80 \pm 27$  °C.

Ti-in-biotite temperatures from peraluminous metapelites with Ti-saturating minerals, but without graphite, can produce reasonable temperatures but they can also be erratic. For instance, biotite from lower-to-upper sillimanite zone (580–650 °C) peraluminous metapelites from western Maine (Guidotti unpublished data) containing magnetite and ilmenite, but not graphite, yield Ti-in-biotite temperatures that underestimate the calibrated temperatures by only  $20 \pm 12$  °C. However, biotite from 31 non-graphitic, ilmenite-bearing, peraluminous metapelites from the Ballachulish contact metamorphic aureole of Scotland will, on average, underestimate the reference temperatures (560–820 °C) by 9 °C, but with a much greater standard deviation ( $\pm 50$  °C) of the calculated temperatures (Pattison 1985, 1987, 1989, 1991, unpublished data; Pattison and Harte 1991; Pattison et al. 2002).

#### Monitor of chemical equilibrium and/or re-equilibration

To use reactions that involve biotite and/or application of the principles of thermodynamics to make inferences on temperature, pressure, or fluid evolution, we need to know that chemical equilibrium involving biotite and coexisting minerals has been maintained. However, establishing that a given biotite, or portion of a biotite grain, has reached equilibrium with a particular set of minerals can be equivocal if not impossible. Equilibrium textures do not necessarily imply chemical equilibrium has been attained or retained (Guidotti et al. 1991). Nonetheless, if equilibrium textures are combined with other chemical equilibrium indicators it is much more likely that equilibrium biotite compositions can be assumed. Chemical criteria such as systematic element partitioning involving exchangeable cations, such as Mg and Fe<sup>2+</sup>, among coexisting phases have long been considered one of the strongest arguments (Deb and Saxena 1976; Stephenson 1979). However, observations of this sort require compositional data for several coexisting minerals in each of a number of samples that equilibrated at roughly the same temperature and pressure.

Whereas demonstrating equilibrium is generally difficult, demonstrating disequilibrium may be quite straightforward. In particular, changes in Ti concentration in biotite may result from disequilibrium and/or development of local equilibrium. Biotite compositions can change quite readily, particularly if a late fluid phase is present. Biotite may be altered or replaced, it may undergo retrogressive cation exchange or it may experience reequilibration due to thermal overprint after cooling. Titanium contents of biotite grains and the degree of homogeneity therefore provide a means to evaluate attainment, retention, and extent of chemical equilibrium.

**Minor biotite alteration.** Sometimes, retrograde reactions involving Ti can be inferred from textural features. For example, it is common for biotite with minor degrees of chloritization to develop oriented sagenitic rutile (Fig. 4). The Ti concentration of the remaining biotite decreases while the Fe content generally increases at the same time (Veblen and Ferry 1983; Shau et al. 1991; Pitra and Guiraud 1996). Application of the Ti-in-biotite geothermometer to such biotite grains will always result in anomalously low temperatures.

**Development of biotite with different colors due to retrogression.** A common observation in upper amphibolite- and granulite-fa-

cies rocks is the presence of biotites with two distinct colors in the same thin section, typically red-brown (Ti-rich) and green (Ti-poor) (Edwards and Essene 1988; Thomson 1992, 2001; Ikeda 1998b; Brown 2002; Waters and Charnley 2002). Texturally, it is not always obvious which color-type of biotite is the most likely equilibrium composition. However, based on this study it is clear that the brown (Ti-rich) biotite most likely represents higher-temperature metamorphic conditions versus the (Ti-poor) green biotite. For example, five samples of granulite-facies cordierite pegmatite from south-central Massachusetts have coexisting red-brown matrix biotite and green biotite next to cordierite (Thomson 1992, 2001). The conditions of metamorphism based on mapped isograds, are 745–775 °C at 6–7 kbar. For three of the red-brown matrix biotites, the Ti-in-biotite geothermometer gives temperatures of 758–771 °C (Fig. 5). Two samples have lower temperatures of 711–715 °C, suggesting some compositional resetting. In contrast, the green biotites next to cordierites yield temperatures well below the 450 °C isotherm, are likely artifacts of retrogression. Garnet-biotite Mg-Fe exchange geothermometry (TWQ 2.02b program, Berman 1991) using red-brown and green biotites result in temperature differences of roughly 50 °C for the red-brown biotites (735–746 °C) and green (692–697 °C). Waters and Charnley (2002) attribute similar compositional relations between red and green biotite to development of local equilibrium on cooling in the presence of a fluid.

**Intergranular and intragranular compositional heterogeneity of biotite.** Cryptic variations in Ti contents of biotite are common when biotite is near other ferromagnesian minerals. These features are manifest in various ways. In low- to medium-grade metapelites, biotite rims next to chlorite can be enriched in Ti and Fe, possibly due to incipient chloritization of the biotite without developing rutile (Henry 1981; Zen 1981). In contrast, distinct local depletion of Ti in biotite near garnet being replaced by biotite is also common in high-grade metapelites (e.g., Ikeda 1998b; García-Casco et al. 2001). Additionally, biotite replacing cordierite in metapelites commonly has higher  $X_{Mg}$  and lower Ti content than the biotite located away from the cordierite (Ikeda 1998b; Waters and Charnley 2002). Waters and Charnley (2002) argued that phenomena of this type represent development of

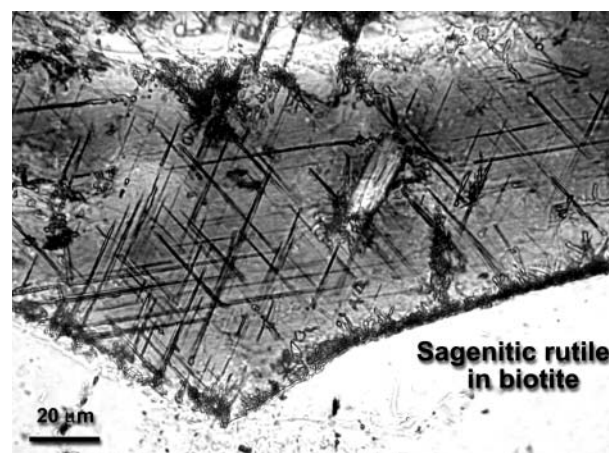


**FIGURE 4.** Partially chloritized biotite with development of sagenitic rutile needles. The sample is a granitic gneiss from the Beartooth Mountains, Montana (Henry, unpublished data).

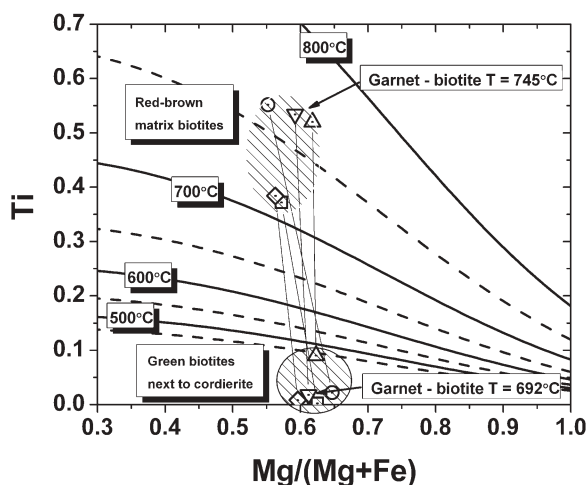


**FIGURE 5.** Ti-in-biotite geothermometry relations for coexisting red-brown and green biotite from cordierite pegmatites from south-central Massachusetts. Tie-lines connect coexisting red-brown and green biotite from five separate samples (data of Thomson 1992, 2001). Note the Mg-enrichment of the green biotites relative to the coexisting red-brown biotite.

local equilibrium.

A more subtle feature is intragranular and intergranular variation in biotite chemistry without obvious textural or color distinctions, particularly in high-grade metamorphic rocks. This type of variation is particularly apparent in the biotite data of Thomson (1992, 2001). Thomson (1992) analyzed 5–10 separate red-brown biotite grains with a range of Mg/(Mg+Fe) contents in 15 samples of peraluminous gneiss from south-central Massachusetts. Within each sample, if the highest Ti analysis is considered, the trend of the biotite data roughly follows the calculated Ti-in-biotite isotherms at ~760–780 °C (Fig. 6). However, if all analyses are considered, each sample shows an array of  $T - \text{Mg}/(\text{Mg} + \text{Fe})$  points trending across the Ti-in-biotite isotherms. The trends involve a decrease in Ti content with a slight increase in Mg/(Mg + Fe). If the trends are extrapolated, they lead to Ti-depleted and significantly Mg-enriched compositions similar to the green biotite data plotted in Figure 5. Besides the data of Thomson (1992), the biotite data of others have similar cryptic intergranular relations in biotites from high-grade metapelitic terrains (Graessner and Schenk 2001; Moraes et al. 2002; Waters and Charnley 2002). All of them likely represent compositional resetting and/or development of localized equilibrium.

### Ti substitution mechanisms

Based on several crystallographic, crystal-chemical, experimental, and theoretical studies, many potential Ti substitution schemes have been proposed (Forbes and Flower 1974; Robert 1976; Holdaway 1980; Dymek 1983; Tronnes et al. 1985; Abrecht and Hewitt 1988; Ahlin 1988; Burt 1988; Brigatti et al. 1991; Cruciani and Zanazzi 1994; Waters and Charnley 2002). All substitutions involve quadrivalent Ti substituting for a lower-charge cation in the M2 site of the octahedral layer requiring coupled substitutions involving multiple cations and possibly anions. The four most widely advocated models for substituting Ti into biotite

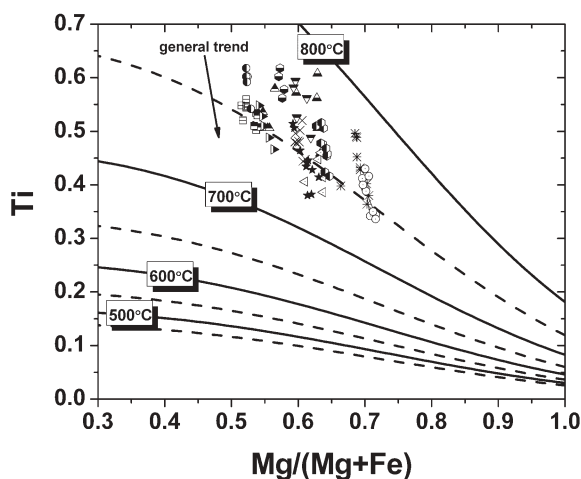


**FIGURE 6.** Cryptic variations of biotite chemistry in individual samples based on multiple biotite analyses among 15 different samples of garnet-cordierite gneiss from south-central Massachusetts (Thomson 1992, 2001).

(Table 3) involve three general types of coupled substitutions: (1) within-octahedral site substitutions resulting in either accumulation of octahedral vacancies via the  $\text{Ti}\square\text{R}_2$  substitution or loss of octahedral Al via the  $\text{TiRAl}_2$  substitution; (2) octahedral-tetrahedral site coupled substitution resulting in enhancement of tetrahedral Al via the  $\text{TiAl}_2\text{R}_1\text{Si}_2$  substitution; or (3) deprotonation (dehydrogenization) resulting in loss of H via the  $\text{TiO}_2\text{R}_1(\text{OH})_2$  substitution. Recently, the latter deprotonation substitution has been strongly favored as the dominant Ti substitution mechanism in high-temperature metapelitic biotites with intermediate Mg/(Mg+Fe) ratios (Waters and Charnley 2002; Cesare et al. 2003). However, it is not clear whether this mechanism is operative across the entire compositional and temperature spectrum.

In theory, each Ti substitution mechanism is influenced by bulk composition, mineral assemblage, biotite crystallochemical constraints, and/or metamorphic fluid compositions in different ways. The  $\text{Ti}\square\text{R}_2$  exchange vector will be most likely enhanced by factors that increase octahedral vacancies in biotite such as the presence of muscovite that may act as a dioctahedral-vacancy saturating phase via the exchange vector  $\text{Al}_2\text{R}_3$  (Labotka 1983; Henry and Guidotti 2002). Titanium introduced with a  $\text{TiRAl}_2$  exchange mechanism will be affected by rock compositions, such that low-Al rocks, those without coexisting Al-saturating phases, should have higher Ti contents in biotite. Conversely, if Ti is introduced via the  $\text{TiAl}_2\text{R}_1\text{Si}_2$  substitution mechanism, low-Al rocks should have lower Ti contents in biotite. The  $\text{TiO}_2\text{R}_1(\text{OH})_2$  exchange vector will be affected by the local activity of  $\text{H}_2\text{O}$  in the metamorphic fluid such that lower  $a_{\text{H}_2\text{O}}$  fluids will lead to more deprotonation and, consequently, higher Ti concentrations in the biotite. Additional biotite substitutions that may indirectly influence the amount of octahedral Ti include  $\text{Al}_2\text{R}_1\text{Si}_1$ ,  $\text{Al}_2\text{R}_3$ ,  $\text{AlOR}_1(\text{OH})_1$  and  $\text{MgFe}_{-1}$ . The  $\text{MgFe}_{-1}$  exchange is particularly significant for Ti substitution. In general, an increase in  $\text{Fe}^{2+}$  in biotite is usually correlated with higher Ti levels, all other factors being constant (Abrecht and Hewitt 1988; Henry and

Guidotti 2002).

**Normalization procedures.** Different biotite normalization procedures establish the number of ions calculated in a biotite formula and, consequently, may influence the interpretation of likely substitution mechanisms. The optimal situation is to normalize biotite on the basis of 24 anions, provided that the biotite is completely analyzed for all cations, anions, and oxidation states. However, because of the inability of the microprobe to measure H contents and the oxidation states of Fe, most biotite analyses are normalized using different assumptions. Four biotite normalization procedures have been proposed for microprobe analyses. (1) The most common procedure is to normalize analyses on the basis of 22 O atoms and assume all Fe is Fe<sup>2+</sup>. The inherent supposition is that (OH)<sup>1-</sup> + F<sup>1-</sup> + Cl<sup>1-</sup> = 4.0. If the biotite is partially deprotonated, the 22 O normalization will underestimate the total number of cations proportional to the amount of deprotonation, and result in a proportional number of apparent octahedral vacancies. Conversely, if some Fe is Fe<sup>3+</sup>, the 22 O normalization will overestimate the total number of cations proportional to the number of Fe<sup>3+</sup> cations. (2) Dymek (1983) considered that Ti and excess octahedral Al was linked to octahedral vacancies and suggested an iterative procedure be used in which the sum of the tetrahedral cations, octahedral cations, Ti and excess octahedral Al is normalized to 14 cations. (3) In contrast, Waters and Charnley (2002) suggested that the number of octahedral vacancies is minor and advocated the deprotonation substitution as the dominant Ti substitution. They use an iterative normalization procedure on the basis of 22 + Ti O atoms. (4) Finally, based on complete biotite analyses, Bohlen et al. (1980) found that there are minor or no octahedral vacancies (<0.05 pfu) in biotites from a granulite-facies sample. They suggest that normalization based on tetrahedral + octahedral cations = 14 may be the most reasonable. All cation-based normalization procedures are independent of H<sub>2</sub>O contents and oxidation states of transition elements.

To examine the influence of normalization on interpretation of substitution schemes, biotite data were normalized on the basis of all four of the normalization schemes. For biotites with <0.3 Ti apfu, the different normalization procedures produce minor changes in the absolute values of cations. When plotted on binary diagrams that are used to test possible substitution schemes there are insignificant changes in the relative positions of the data. For those biotites with >0.3 Ti apfu, there is a proportionately greater shift in the calculated values of the cations at the higher Ti contents, although the general compositional trends are maintained. Consequently, for the following discussion of Ti substitution mechanisms, the 22 O normalization procedure is used for the lower-Ti peraluminous biotite of the staurolite/lower sillimanite zone metapelites, but in the higher-Ti biotite of the

amphibolite/granulite-facies metaluminous rocks, a 14 cation normalization is used.

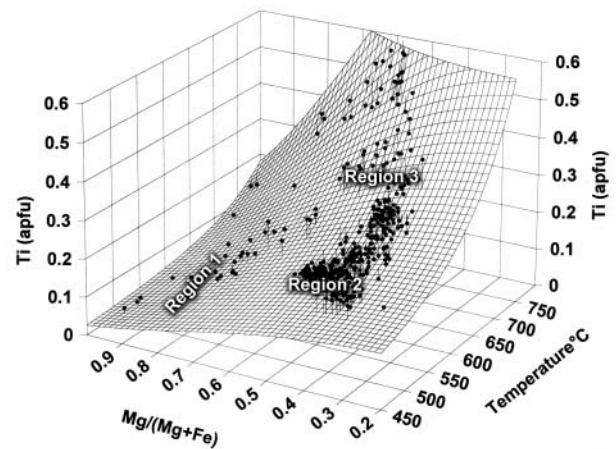
**Ti substitutions in peraluminous biotite.** The biotite Ti-saturation surface has 3 general regions that display noteworthy changes in slope of the Ti- $X_{Mg}$ - $T$  relations: Region 1, the steeper-sloped Mg-richer region that starts at roughly  $X_{Mg}$  > 0.65; Region 2, the relatively shallowly sloped region at the lower temperature (<600 °C) and intermediate  $X_{Mg}$  portion of the surface; and Region 3, the higher temperature region (>600 °C) (Fig. 7). Rather than relying on the surface fit with any biases that might be introduced, we used a subset of the actual biotite data from western Maine to assess likely Ti substitutions in each of these regions. For this more detailed examination, biotite data are limited to staurolite zone and transition/lower sillimanite zone samples. These zones were chosen because they exhibit a significant transition in the character of the Ti systematics in biotite, they contain the largest numbers of analyses, and they have equilibrated in a relatively restricted temperature range, 545–580 °C for the staurolite zone and 580–620 °C for the transition/lower sillimanite zone.

Figure 8 shows four binary composition diagrams and the trends that would result from different exchange vectors. In Region 1, the Mg-rich portion of the diagram, there is a general inverse relationship between Ti and Mg/(Mg + Fe) ratios of biotite in each metamorphic zone (Fig. 8a). In addition, Ti is negatively correlated with the sum of the total divalent cations (Mg + Fe + Mn) and Si contents, and is positively correlated with the Al<sub>total</sub> (Figs. 8b, 8c, 8d). This trend in data is most consistent with variation due to the exchange vector TiAl<sub>2</sub>R<sub>1</sub>Si<sub>2</sub>. These relationships are likely controlled by crystal-chemical factors in that substitution of relatively small Ti<sup>4+</sup> cations in the octahedral layer and Al<sup>3+</sup> cations in the tetrahedral layer compensates for any octahedral-tetrahedral layer misfit resulting from substitution of larger Fe<sup>2+</sup> cations for smaller Mg<sup>2+</sup> cations in the octahedral layer (Guidotti et al. 1977). This produces a decrease in the average layer distortion and results in the M1 and M2 octahedral sites becoming more distinct, with M1 being more distorted and larger than M2 (Brigatti and Guggenheim 2002). In Region 2, staurolite zone biotite data at intermediate  $X_{Mg}$ , inverse relationships among

**TABLE 3.** Most likely substitution schemes and exchange vectors for incorporation of Ti into biotite

Site substitution	Exchange vector
$2^{\vee}R^{2+} = {}^{\vee}Ti + {}^{\vee}\square$	Ti□ R <sub>2</sub>
$2^{\vee}Al = {}^{\vee}Ti + {}^{\vee}R^{2+}$	TiAl <sub>2</sub>
${}^{\vee}R^{2+} + 2^{\vee}Si = {}^{\vee}Ti + 2^{\vee}Al$	TiAl <sub>2</sub> R <sub>1</sub> Si <sub>2</sub>
${}^{\vee}R^{2+} + 2(OH)^{1-} = {}^{\vee}Ti + 2O^{2-}$	TiO <sub>2</sub> R <sub>1</sub> (OH) <sub>2</sub>

\*  ${}^{\vee}R^{2+}$  represents the sum of the divalent cations in the octahedral sites and  ${}^{\vee}\square$  represents the octahedral site vacancies.



**FIGURE 7.** Titanium saturation surface for natural peraluminous biotites at 4–6 kbar highlighting different regions on interest.

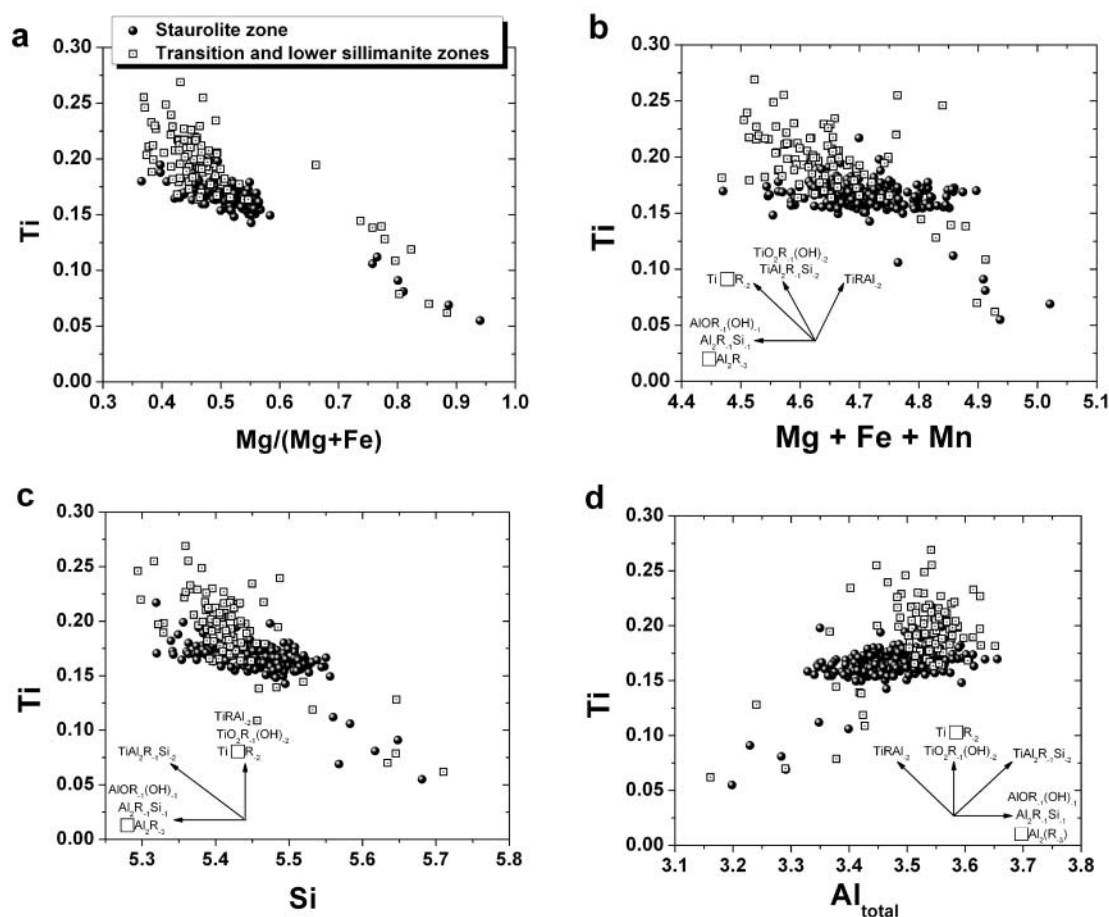


**FIGURE 8.** Biotite data from western Maine for the staurolite and transition/lower sillimanite zones normalized on a 22 O basis. (a) Ti – Mg/(Mg + Fe) relations. Note break in slope of data trend at the Mg-rich end of the diagram. (b) Ti – (Mg + Fe + Mn) relations. The arrows represent the direction of the possible exchange vectors. (c) Ti-Si relations. (d) Ti- $Al_{total}$  relations.

Ti and  $X_{Mg}$ , sum of the total divalent cations (Mg + Fe + Mn) and Si contents persist, but are much less pronounced (Figs. 8b, 8c, 8d). This relationship is most compatible with the  $TiAl_2R_1Si_2$  exchange. However, the principal variation of the data is in the total divalent cations (Mg + Fe + Mn), Si, and  $Al_{total}$  contents and is most consistent with the exchange vectors  $Al_2R_1Si_1$ ,  $AlOR_1(OH)_1$  and  $Al_2R_3$ . In Region 3, transition and lower sillimanite zone biotite data at intermediate  $X_{Mg}$ , Ti is dispersed to higher values and is best explained by a significant amount of substitution due to deprotonation described by  $TiO_2R_1(OH)_2$  (Figs. 8b, 8c, 8d).

The shift in the Ti substitution mechanism above the staurolite zone suggests that there may be a fundamental change in the metamorphic environment at higher metamorphic grades. The increasing importance of the  $TiO_2R_1(OH)_2$  exchange implies that biotite above the staurolite zone is being exposed to metamorphic fluids with lower  $a_{H_2O}$ . In fact, there is direct evidence for deprotonation in higher-grade biotites from western Maine. Dyar et al. (1991) measured H contents in a subset of biotites from the calibration data set and found that biotites from higher-grade zones, particularly above the staurolite zone, were

significantly depleted in H. The lower  $a_{H_2O}$  environment can be understood by considering the likely metamorphic fluids in equilibrium with graphite in the COHS system. Graphite-bearing metapelites that undergo dehydration reactions generally produce fluids that have H/O ratios of 2:1 i.e., they approach the  $H_2O$  maximum for a given temperature, with the balance of the fluid being composed of other C- and S-bearing species (Ohmoto and Kerrick 1977; Connolly and Cesare 1993). Calculation of the proportions of species in a COHS metamorphic fluid demonstrate that as temperature increases, the amounts of other species reduce the maximum amount of  $H_2O$ . As such, at temperatures below 550 °C at 4 kbar there are only 3–5% other species at the  $H_2O$  maximum (Connolly and Cesare 1993). However, above 550 °C, the maximum  $X_{H_2O}$  decreases significantly from 0.92 at 600 °C to 0.82 at 700 °C to 0.73 at 800 °C. In theory, this decrease in  $X_{H_2O}$  will enhance the deprotonation exchange reaction  $TiO_2R_1(OH)_2$  and greater amounts of Ti should be incorporated in the biotite. Further, if there are aqueous metamorphic fluids with high salinity, the  $a_{H_2O}$  will also be significantly reduced (Aranovich and Newton 1998) and Ti-deprotonation exchange will likely occur in the coexisting biotites. In contrast, if the

rocks do not contain graphite, the maximal amounts of  $H_2O$  in the metamorphic fluid could be higher than in graphite-bearing rocks and any influence of the deprotonation exchange reaction  $TiO_2R_{-1}(OH)_{-2}$  may be reduced so that biotite Ti contents and the Ti-in-biotite temperatures will be lower. This feature may help to explain the tendency for non-graphitic rocks to yield somewhat lower temperatures.

**Ti substitutions in low-Al biotite.** Ti substitution mechanisms can be extended beyond peraluminous biotites by considering an additional extensive biotite data set from high-grade metaluminous bulk compositions. Harlov and Forster (2002) include a detailed biotite data set in their study that reported on a gneiss terrane that has experienced a high-grade metamorphic overprint at  $\sim 800^\circ C$  and 8 kbar under locally variable  $a_{H_2O}$  conditions. A hornblende-bearing metatonalite from the Seward Peninsula, Alaska, locally develops an 80 cm dehydration zone next to a marble layer, apparently associated with a  $CO_2$ -rich and low  $a_{H_2O}$  fluid. The host rock metatonalite has a uniform assemblage of hornblende + biotite + plagioclase + quartz + pyrrhotite + graphite, but no Ti-saturating mineral (ilmenite or rutile). The dehydration zone, lacking horn-

blende, develops in a zone within 50 cm of the marble unit and has an assemblage of orthopyroxene + clinopyroxene + Ti-rich biotite + plagioclase + quartz + minor K-feldspar + pyrrhotite. There is a 30 cm wide transition zone that represents partial dehydration with some hornblende remaining. The factors that are likely to influence biotite chemistry include: (1) the rocks do not contain a Ti-saturating phase and, consequently, the biotite will be unsaturated with respect to Ti and subject to variation in bulk composition; (2) there is graphite present but no  $Fe^{3+}$ -saturating phase, hence,  $Fe^{3+}$  should be relatively low and constant; (3) the rocks do not contain an Al-saturating phase so that Al levels will be lower than peraluminous metapelites; and (4) the biotite will be primarily influenced by local variation in  $a_{H_2O}$  because they are derived from an isothermal and isobaric setting. A total of 470 biotite analyses from 12 samples are available with multiple biotite analyses from the same grain and from several grains from the same sample.

The Ti –  $Mg/(Mg + Fe)$  relations illustrate that there are two clusters of data (Fig. 9a). (1) The lower-Ti biotite samples from the amphibolite and transition zone exhibit a range of  $Mg/(Mg$

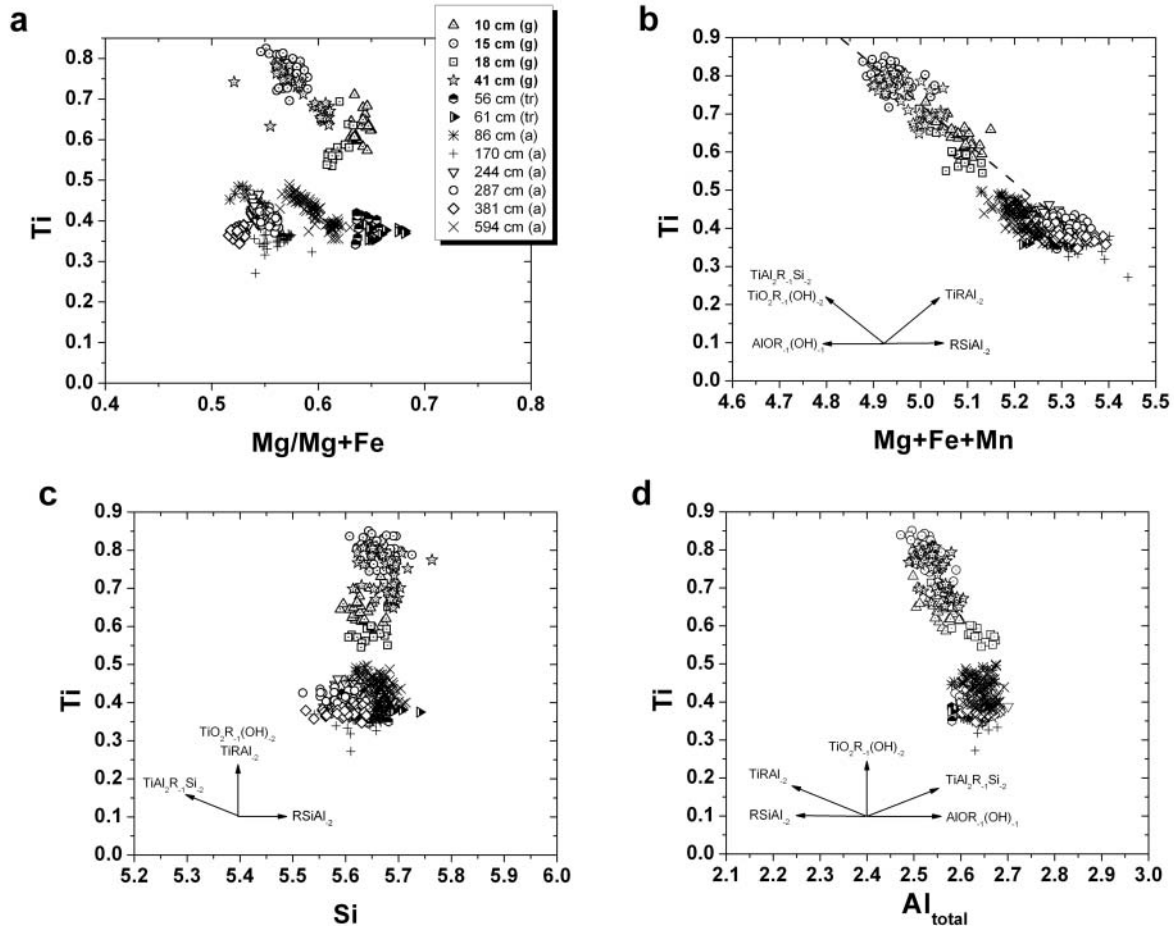


**FIGURE 9.** Isothermal biotite data from low-Al biotites from metaluminous amphibolites to mafic granulites from Alaska (Harlov and Forster 2002) normalized on a 14 cation basis. The estimated metamorphic conditions are  $800^\circ C$  and 8 kbar. (a) Ti –  $Mg/(Mg + Fe)$  relations. Each of the 12 samples has multiple biotite analyses (470 total analyses) with the distance (in cm) from the marble unit indicated next to the symbol. The g next to the sample number indicates a sample with a granulite-facies assemblage, t represents a transitional sample and a represents a sample with amphibolite-facies assemblage. (b) Ti –  $(Mg + Fe + Mn)$  relations. The arrows represent the direction of the possible exchange vectors. The dashed line is a reference line with a slope of 1. (c) Ti-Si relations. (d) Ti- $Al_{total}$  relations.

+ Fe) (0.52–0.68) and Ti (0.27–0.49 apfu) among the different samples. Application of the Ti-in-biotite geothermometer to this group of data yields a maximum apparent temperature of 745 °C, representing a minimum temperature estimate because of the lack of a Ti-saturating phase. Biotite data from some of the samples exhibit significant dispersion, with a common trend being a decrease in Ti associated with an increase in Mg/(Mg + Fe) ratio, a pattern consistent with partial resetting during cooling (Fig. 6). (2) The high-Ti biotite samples are from the dehydrated mafic granulite zone within 50 cm of the marble. The biotite has a range of Mg/(Mg + Fe) (0.53–0.65) similar to the low-Ti data, but with significantly higher Ti (0.53–0.82 apfu). Apparent Ti-in-biotite temperatures are higher than the lower-Ti samples, with a range of 775–810 °C, close to the regional temperature estimates, but likely related to the manner in which Ti substitutes in lower-Al biotite under variable  $a_{\text{H}_2\text{O}}$  conditions.

A series of binary composition diagrams help define the most likely substitutions in the isothermal low-Al biotites with variable  $a_{\text{H}_2\text{O}}$ . In addition to variable Mg/(Mg + Fe) ratios, the lower-Ti biotites also exhibit a minor dispersion of data roughly parallel to the  $\text{Al}_2\text{R}_1\text{Si}_1$  and  $\text{AlOR}_1(\text{OH})_1$  vectors (Fig. 9b, 9c, 9d). In the granulite facies samples with higher-Ti biotite, the increase in Ti in biotite has a slope of roughly 1.0 when plotted against Mg + Fe + Mn (Fig. 9b) and a slightly positive slope plotted against Si (Fig. 9c). The Ti exchange vector that best satisfies both of these criteria is  $\text{TiO}_2\text{R}_1(\text{OH})_2$ . The separation between the low-Ti biotite and the maximum values of the high-Ti groups is approximately 0.4 Ti apfu, implying that the operation of the  $\text{TiO}_2\text{R}_1(\text{OH})_2$  vector by 0.4 units and a resulting deprotonation of the highest-Ti biotites by about 0.8 H apfu. However, the Ti- $\text{Al}_{\text{total}}$  diagram (Fig. 9d) shows an additional inverse relationship between Ti and Al, implying another exchange takes place that reduces the amount of Al by about 1 apfu for each 0.4 Ti apfu. The substitution that is most consistent with these relationships is the  $\text{RSi}(\text{Al}_2)$  vector. Consequently, the major changes between low- and high-Ti samples can be defined by a combination of 0.4  $\text{TiO}_2\text{R}_1(\text{OH})_2$  and 0.05  $\text{RSi}(\text{Al}_2)$  vectors, and a resultant cumulative exchange vector of  $\text{Ti}_{0.4}\text{O}_{0.8}\text{Si}_{0.05}(\text{R}_{0.35}\text{Al}_{0.1}(\text{OH})_{0.8})$ . The reduction of Al in both the octahedral and tetrahedral layers in conjunction with the introduction of the larger divalent cations in the octahedral layer and smaller Si cation in the tetrahedral layer probably represents the response of the biotite structure to introduction of the smaller Ti into the octahedral layer.

#### SUMMARY STATEMENT

The Ti-saturation surface generated for biotites from peraluminous metapelites at low-to-medium pressures contains useful information with petrologic and crystallographic implications. A reformulation of the surface fit expression results in an empirical Ti-in-biotite geothermometer for biotites in peraluminous metamorphic rocks. The geothermometer is valid over a range of 480 to 800 °C and has an estimated precision of  $\pm 24$  °C. Further, the systematics of Ti in biotite provides a means to assess the approach to chemical equilibrium of biotite in metamorphic rocks. Finally, the Ti-saturation surface provides evidence that Ti is incorporated into biotite by at least two substitution mechanisms. In magnesian biotite, Ti primarily substitutes via a Ti-tschermaks substitution controlled by octahedral-tetrahedral

layer misfit. However, at intermediate  $X_{\text{Mg}}$ , Ti-deprotonation substitution becomes the dominant mechanism for Ti incorporation, particularly at metamorphic grade above the staurolite zone where there is significant reduction of activity of  $\text{H}_2\text{O}$  in the metamorphic fluid from graphite-bearing metapelites. This study highlights the petrologic mineralogy approach, as described by Guidotti and Sassi (2002), in which natural solid-solution minerals, constrained by phase-rule variance considerations and equilibration, are used to provide mineralogic and petrologic insights not generally available via typical experimental or crystallography studies.

#### ACKNOWLEDGMENTS

We are pleased to acknowledge all of our colleagues who have contributed to the biotite data set over the years including Kathy Bussa, Jack Cheney, Paul Conatore, Barb Dutrow, Angela LaGrange, Steve Lonker, David Pattison, and Virginia Peterson. We are grateful to the many of the people cited in terms of our sources of data as in many cases they provided us electronic files of their data, thereby making it much easier for us to process. Amber Hawkins at the University of Maine did much of this processing. Finally, discussions about Ti in biotite with Bernardo Cesare, Darby Dyar, and Ed Grew have been helpful in many ways. Insightful reviews by Dexter Perkins, Tom Hoisch, and Ted Labotka greatly improved the final manuscript.

#### REFERENCES CITED

- Abrecht, J. and Hewitt, D.A. (1988) Experimental evidence on the substitution of Ti in biotite. *American Mineralogist*, 73, 1275–1284.
- Ahlin, S. (1988) Interpretation of biotite-garnet partitioning data from two Sveco-karelian metamorphic rock units. *Lithos*, 22, 25–29.
- Alias, G., Sandiford, M., Hand, M., and Worley, B. (2002) The P-T record of synchronous magmatism, metamorphism and deformation at Petrel Cove, southern Adelaide Fold Belt. *Journal of Metamorphic Geology*, 20, 351–363.
- Aranovich, L.Y. and Newton, R.C. (1998) Reversed determination of the reaction: Phlogopite + quartz = enstatite + potassium feldspar +  $\text{H}_2\text{O}$  in the ranges 750–875 °C and 2–12 kbar at low  $\text{H}_2\text{O}$  activity with concentrated KCl solutions. *American Mineralogist*, 83, 193–204.
- Arima, M. and Edgar, A.D. (1981) Substitution mechanisms and solubility of titanium in phlogopites from rocks of probable mantle origin. *Contributions to Mineralogy and Petrology*, 77, 288–295.
- Berman, R.G. (1991) Thermobarometry using multiequilibrium calculations: a new technique with petrologic applications. *Canadian Mineralogist*, 29, 833–855.
- Bohlen, S.R., Peacor, D.R., and Essene, E.J. (1980) Crystal chemistry of a metamorphic biotite and its significance in water barometry. *American Mineralogist*, 65, 55–62.
- Brigatti, M.F. and Guggenheim, S. (2002) Mica crystal chemistry and the influence of pressure, temperature, and solid solution on atomistic models. In A. Mot-tana, F.P. Sassi, J.B. Thompson Jr., and S. Guggenheim, Eds., *Micas: Crystal Chemistry and Metamorphic Petrology*, 46, 1–98. Reviews in Mineralogy and Geochemistry, Mineralogical Society of America, Washington, D.C.
- Brigatti, M.F., Galli, E., and Poppi, L. (1991) Effect of Ti substitution in biotite-1M crystal chemistry. *American Mineralogist*, 76, 1174–1183.
- Brown, M. (2002) Prograde and retrograde processes in migmatites revisited. *Journal of Metamorphic Geology*, 20, 25–40.
- Burt, D.M. (1988) Vector representations of phyllosilicate compositions. In S.W. Bailey, Ed., *Hydrous Phyllosilicates (exclusive of micas)*, 19, 561–599. Reviews in Mineralogy, Mineralogical Society of America, Washington, D.C.
- Cesare, B., Cruciani, G., and Russo, U. (2003) Hydrogen deficiency in Ti-rich biotite from anatectic metapelites (El Joyazo, SE Spain): crystal-chemical aspects and implications for high-temperature petrogenesis. *American Mineralogist*, 88, 583–595.
- Connolly, J.A.D. and Cesare, B. (1993) C-O-H-S fluid composition and oxygen fugacity in graphitic metapelites. *Journal of Metamorphic Geology*, 11, 379–388.
- Cruciani, G. and Zanazzi, P.F. (1994) Cation partitioning and substitution mechanisms in 1M phlogopite: a crystal-chemical study. *American Mineralogist*, 79, 289–301.
- Deb, M. and Saxena, S.K. (1976) A method of appraisal of chemical equilibrium - application to terrestrial and lunar rocks. *Lithos*, 9, 225–234.
- DeYoreo, J.J., Lux, D.R., Guidotti, C.V., Decker, E.R., and Osberg, P.H. (1989) The Acadian thermal history of western Maine, *Journal of Metamorphic Geology*, 7, 169–170.
- Dutrow, B.L. (1985) A Staurolite Trilogy: III. Evidence for Multiple Metamorphic Events in the Farmington Quadrangle, Maine. Ph.D. Thesis, Southern Method-

- ist University, Dallas, TX.
- Dyar, M.D., Colucci, M.T., and Guidotti, C.V. (1991) Forgotten major elements: Hydrogen and oxygen variation in biotite from metapelites. *Geology*, 19, 1029–1032.
- Dymek, R.F. (1983) Titanium, aluminum and interlayer cation substitutions in biotite from high-grade gneisses, West Greenland. *American Mineralogist*, 68, 880–899.
- Edwards, R.L. and Essene, E.J. (1988) Pressure, temperature and C-O-H fluid fugacities across the amphibolite-granulite facies transition, NW Adirondack Mountains, NY. *Journal of Petrology*, 29, 39–73.
- Engel, A.E.J. and Engel, C.G. (1960) Progressive metamorphism and granulitization of the major paragneiss, northwest Adirondack Mountains, New York, Part 2. *Mineralogy. Bulletin of the Geological Society of America*, 71, 1–58.
- Ferry, J.M. (1981) Petrology of graphitic sulfide-rich schists from south-central Maine: an example of desulfidation during prograde regional metamorphism. *American Mineralogist*, 66, 908–930.
- Florence, F.P., Spear, F.S., and Kohn, M.J. (1993) *P-T* paths from northwestern New Hampshire: metamorphic evidence from stacking in a thrust/nappe complex. *American Journal of Science*, 293, 939–979.
- Forbes, W.C. and Flower, M.F.J. (1974) Phase relations of titan-phlogopite,  $K_2MgTiAl_3Si_4O_{20}(OH)_2$ : A refractory phase in the upper mantle?: *Earth Planetary Science Letters*, 22, 60–66.
- García-Casco, A., Torres-Roldán, R.L., Millán, G., Monié, P., and Haissen, F. (2001) High-grade metamorphism and hydrous melting of metapelites in the Pinos terrane (W Cuba): Evidence for crustal thickening and extension in the northern Caribbean collisional belt. *Journal of Metamorphic Geology*, 19, 699–715.
- Graessner, T. and Schenk, V. (2001) An exposed Hercynian deep crustal section in the Sila Massif of northern Calabria: Mineral Chemistry, petrology and a *P-T* path of granulite-facies metapelitic migmatites and metabasites. *Journal of Petrology*, 42, 931–961.
- Guidotti, C.V. (1970a) The mineralogy and petrology of the transition from lower to upper sillimanite zone in the Oquossoc area, Maine. *Journal of Petrology*, 11, 277–336.
- — — (1970b) Metamorphic petrology, mineralogy, and polymetamorphism in a portion of N.W. Maine. In Boone, G.M., editor, Guidebook for field trips in the Rangeley Lakes—Dead Rivers Basin region, Western Maine. New England Intercollegiate Geology Conference, 62<sup>nd</sup> Annual Meeting, Field Trip B2, 1–23.
- — — (1974) Transition from staurolite to sillimanite zone, Rangeley quadrangle, Maine. *Geological Society of America Bulletin*, 85, 475–490.
- — — (1984) Micas in metamorphic rocks. In S.W. Bailey, Ed., *Micas*, 13, 357–467. Reviews in Mineralogy, Mineralogical Society of America, Washington, D.C.
- — — (1985) Metamorphic map of Maine. In P.H. Osberg, A.M. Hussey II, and G.M. Boone, Eds., *Geologic map of Maine*. Maine Geological Survey, Augusta, Maine.
- — — (1989) Metamorphism in Maine: an overview. In R.D. Tucker and R.G. Marviny, Eds., *Studies in Maine Geology*, 3, 1–17. Maine Geological Survey, Augusta, Maine.
- Guidotti, C.V. and Dyar, M.D. (1991) Ferric iron in metamorphic biotite and its petrologic and crystallographic implications. *American Mineralogist*, 76, 161–175.
- Guidotti, C.V. and Sassi, F.P. (2002) Constraints on studies of metamorphic K-Na white micas. In A. Mottana, F.P. Sassi, J.B. Thompson Jr., and S. Guggenheim, Eds., *Micas: Crystal Chemistry and Metamorphic Petrology*, 46, 419–448. Reviews in Mineralogy and Geochemistry, Mineralogical Society of America, Washington, D.C.
- Guidotti, C.V., Cheney, J.T., and Guggenheim, S. (1977) Distribution of titanium between coexisting muscovite and biotite in pelitic schists from northwestern Maine. *American Mineralogist*, 62, 438–448.
- Guidotti, C.V., Cheney, J.T., and Henry, D.J. (1988) Compositional variation of biotite as a function of metamorphic reactions and mineral assemblage in the pelitic schists of western Maine: *American Journal of Science - Wones Memorial Volume*, 288A, 270–292.
- Guidotti, C.V., Teichmann, F., and Henry, D.J. (1991) Evidence for equilibrium chlorite in the polymetamorphic metapelites of the Rangeley area, western Maine. *American Mineralogist*, 76, 867–879.
- Harlov, D.E. and Forster, H. (2002) High-grade fluid metasomatism on the local and regional scale: the Seward Peninsula, Alaska, and the Val Strona di Omegna, Ivrea-Verbano Zone, Northern Italy. Part I. Petrography and silicate mineral chemistry. *Journal of Petrology*, 43, 769–799.
- Henry, D.J. (1981) Sulfide-silicate relations of the staurolite grade pelitic schists, Rangeley quadrangle, Maine. Ph.D. thesis, University of Wisconsin—Madison, Madison, Wisconsin.
- Henry, D.J. and Guidotti, C.V. (2002) Ti in biotite from metapelitic rocks: Temperature effects, crystallochemical controls and petrologic applications. *American Mineralogist*, 87, 375–382.
- Holdaway, M.J. (1980) Chemical formulae and activity models for biotite, muscovite and chlorite applicable to pelitic metamorphic rocks. *American Mineralogist*, 65, 711–719.
- Holdaway, M.J., Guidotti, C.V., Novak, J.M., and Henry, W.E. (1982) Polymetamorphism in medium- to high-grade pelitic metamorphic rocks, west-central Maine. *Geological Society of America Bulletin*, 93, 572–584.
- Holdaway, M.J., Dutrow, B.L., and Hinton, R.W. (1988) Devonian and Carboniferous metamorphism in west-central Maine: the muscovite-almandine geobarometer and the staurolite problems revisited. *American Mineralogist*, 73, 20–47.
- Ibarguchi, G.J.I. and Martinez, F.J. (1982) Petrology of garnet-cordierite-sillimanite gneisses from the El Tormentes thermal dome, Iberian Hercynian foldbelt (W Spain). *Contributions to Mineralogy and Petrology*, 80, 14–24.
- Ikeda, T. (1998a) Phase equilibria and the pressure-temperature path of the highest-grade Ryoke metamorphic rocks in the Yanai district, SW Japan. *Contributions to Mineralogy and Petrology*, 132, 321–335.
- — — (1998b) Progressive sequence of reactions of the Ryoke metamorphism in the Yanai district, southwest Japan: the formation of cordierite. *Journal of Metamorphic Geology*, 16, 39–52.
- Johnson, T.E., Brown, M., and Solar, G.S. (2003) Low-pressure subsolidus and suprasolidus phase equilibria in the MnNCKFMASH system. Constraints on conditions of regional metamorphism in western Maine, northern Appalachians. *American Mineralogist*, 88, 624–638.
- Kwak, T.A.P. (1968) Ti in biotite and muscovite as an indication of metamorphic grade in almandine amphibolite facies rocks from Sudbury, Ontario. *Geochimica et Cosmochimica Acta*, 32, 1222–1229.
- Labotka, T.C. (1983) Analysis of the compositional variations of biotite in pelitic hornfels from northeastern Minnesota. *American Mineralogist*, 68, 900–914.
- Moraes, R., Brown, M., Fuck, R.A., Camargo, M.A., and Lima, T.M. (2002) Characterization and *P-T* evolution of melt-bearing ultrahigh-temperature granulites: an example from the Anápolis-Ataúçu Complex of the Brasília Fold Belt, Brazil. *Journal of Petrology*, 43, 1673–1705.
- Ohmoto, H. and Kerrick, D.M. (1977) Devolatilization equilibria in graphitic schists. *American Journal of Science*, 277, 1013–1044.
- Patiño Douce, A.E. (1993) Titanium substitution in biotite: an empirical model with applications to thermometry,  $O_2$  and  $H_2O$  barometries, and consequences for biotite stability. *Chemical Geology*, 108, 133–162.
- Patiño Douce, A.E. and Harris, N. (1998) Experimental constraints on Himalayan anatexis. *Journal of Petrology*, 39, 689–710.
- Patiño Douce, A.E. and Johnston, A.D. (1991) Phase equilibria and melt productivity in the pelitic system: implications for the origin of peraluminous granulitoid and aluminous granulites. *Contributions to Mineralogy and Petrology*, 107, 202–218.
- Pattison, D.R.M. (1985) Petrogenesis of pelitic rocks in the Ballachulish thermal aureole. Unpublished Ph.D. thesis, University of Edinburgh, 590 pp.
- — — (1987) Variations in  $Mg/(Mg + Fe)$ , F, and  $(Fe,Mg)Si = 2Al$  in pelitic minerals in the Ballachulish thermal aureole, Scotland. *American Mineralogist*, 72, 255–272.
- — — (1989) *P-T* conditions and the influence of graphite on pelitic phase relations in the Ballachulish aureole, Scotland. *Journal of Petrology*, 30, 1219–1244.
- — — (1991) *P-T-a(H\_2O)* conditions in the thermal aureole. In G. Voll, J. Topel, D.R.M. Pattison, and F. Seifert, Eds., *Equilibrium and kinetics in contact metamorphism: The Ballachulish Igneous Complex and its aureole*. Springer Verlag, Heidelberg.
- Pattison, D.R.M. and Harte, B. (1991) Petrography and mineral chemistry of pelites. In G. Voll, J. Topel, D.R.M. Pattison, and F. Seifert, Eds., *Equilibrium and kinetics in contact metamorphism: The Ballachulish Igneous Complex and its aureole*. Springer Verlag, Heidelberg.
- Pattison, D.R.M., Spear, F.S., DeBuhr, C.L., Cheney, J.T., and Guidotti, C.V. (2002) Thermodynamic modeling of the reaction muscovite + cordierite  $\rightarrow$   $Al_2SiO_5$  + biotite + quartz +  $H_2O$ : constraints from natural assemblages and implications for the metapelitic petrogenetic grid. *Journal of Metamorphic Geology*, 20, 99–118.
- Peterson, V.L. (1992) Structure, petrology, and tectonic implications of highly strained rocks along the west margin of the Acadian granulite-facies high, south-central Massachusetts: Ph.D. thesis, University of Massachusetts, Amherst, Massachusetts.
- Pitra, P. and Guiraud, M. (1996) Probable anticlockwise *P-T* evolution in extending crust: Hlinsko region, Bohemian Massif. *Journal of Metamorphic Petrology*, 14, 49–60.
- Pressley, R.A. and Brown, M. (1999) The Phillips pluton, Maine, USA: evidence for heterogeneous crustal sources for granitic ascent and emplacement mechanisms in convergent orogens. *Lithos*, 49, 335–366.
- Robert, J.L. (1976) Titanium solubility in synthetic phlogopite solid solutions. *Chemical Geology*, 17, 213–227.
- Shau, Y., Yang, H., and Peacor, D.R. (1991) On oriented titanite and rutile inclusions in sagenitic biotite. *American Mineralogist*, 76, 1205–1217.
- Shearer, C.K., Papike, J.J., Simmons, S.B., and Laul, J.C. (1986) Pegmatite-wall-rock interactions, Black Hills, South Dakota: Interaction between pegmatite-derived fluids and quartz-mica schist wallrock. *American Mineralogist*, 71, 518–539.
- Spear, F.S. and Cheney, J.T. (1989) A petrogenetic grid for pelitic schists in the system  $SiO_2-Al_2O_3-FeO-MgO-K_2O-H_2O$ . *Contributions to Mineralogy and*

- Petrology, 101, 149–164.
- Spear, F.S., Kohn, M.J. and Cheney, J.T. (1999) P-T paths from anatectic pelites. *Contributions to Mineralogy and Petrology*, 134, 17–32.
- Stephenson, N.C.N. (1979) Coexisting garnets and biotites from Precambrian gneisses of the south coast of Western Australia. *Lithos*, 12, 73–87.
- Symmes, G.H. and Ferry, J.M. (1995) Metamorphism, fluid flow and partial melting in pelitic rocks from the Onawa contact aureole, central Maine, USA. *Journal of Petrology*, 36, 587–612.
- Thomson, J.A. (1992) Petrology of high-grade schists, gneisses, and cordierite pegmatites in south-central Massachusetts: Ph.D. thesis, University of Massachusetts, Amherst, Massachusetts.
- — — (2001) A counterclockwise P-T path for anatectic pelites, south-central Massachusetts. *Contributions to Mineralogy and Petrology*, 141, 623–641.
- Tracy, R.J. (1978) High grade metamorphic reactions and partial melting in pelitic schist, west-central Massachusetts. *American Journal of Science*, 278, 150–178.
- Tracy, R.J. and Robinson, P. (1988) Silicate-sulfide-oxide-fluid reactions in granulite-grade pelitic rocks, central Massachusetts. *American Journal of Science*, 288-A, 45–74.
- Tronnes, R.G., Edgar, A.D., and Arima, M. (1985) A high pressure-high temperature study of TiO<sub>2</sub> solubility in Mg-rich phlogopite: Implications to phlogopite chemistry. *Geochimica et Cosmochimica Acta*, 49, 2323–2329.
- Veblen, D.R. and Ferry, J.M. (1983) A TEM study of the biotite-chlorite reaction and comparison with petrologic observation: *American Mineralogist*, 68, 1160–1168.
- Waters, D.J. and Charnley, N.R. (2002) Local equilibrium in polymetamorphic gneiss and the titanium substitution in biotite. *American Mineralogist*, 87, 383–396.
- Waters, D.J. and Whales, C.J. (1984) Dehydration melting and the granulite transition in metapelites from southern Namaqualand, S. Africa. *Contributions to Mineralogy and Petrology*, 88, 269–275.
- Zen, E. (1981) Metamorphic mineral assemblages of slightly calcic pelitic rocks in and around the Taconic Allochthon, southwestern Massachusetts and adjacent Connecticut and New York. *Geological Survey Professional Paper* 1113, 128 p.

MANUSCRIPT RECEIVED SEPTEMBER 30, 2004

MANUSCRIPT ACCEPTED OCTOBER 11, 2004

MANUSCRIPT HANDLED BY THEODORE LABOTKA